UNIVERSITY OF RWANDA

EAST AFRICAN INSTITUTE FOR FUNDAMENTAL RESEARCH

INTERNATIONAL CENTER FOR THEORETICAL PHYSICS

Seismicity in East Africa: a statistical analysis

Aloys RUBWIRIZA
Student number: 213001640

Thesis Submitted in Partial Fulfillment of the Academic Degree of
Master of Science
in
Physics of the Solid Earth (Geophysics)

Supervisor: Dr. Catherine Mériaux

February 1, 2021

Kigali - Rwanda

Declaration

I, **Aloys RUBWIRIZA**, hereby declare and confirm that this research thesis entitled "*Seismicity in East Africa: a statistical analysis*" is my original work and it has never been submitted or published anywhere by any person to any University or other Institution of high learning for academic publication for any award. This Thesis was conducted under the supervision of
Dr. Catherine Mériaux from the School of Earth, Atmosphere and Environment, Monash University, Australia and the East African Institute for Fundamental Research (ICTP-EAIFR),University of Rwanda, Rwanda.

February 1, 2021

Aloys RUBWIRIZA

Dedication

To my lovely family, my future lovely wife ”Santa Kevine UMUTONIWASE” and my supervisor **Dr. Catherine Mériaux**.

Approval

This dissertation was conducted under the guidance and supervision of

Supervisor name:...........................

Signature:.................................

Date:......................................

Abstract

In this thesis, we present a statistical analysis of the seismicity along the East African Rift. We also distinguished the different branches of the rift: the Eastern branch (EB), the Western branch (WB), the Main Ethiopian rift (MER) and the Southeastern branch (SEB). We used QGIS to generate the maps showing the seismicity distribution in all above segments. We systematically analyzed, both in the entire region and in the different branches, the distribution of the seismicity as a function of time, depth, magnitude, latitude and longitude. To do so, we built a home-made Python script. We generated simple and bi-variate histograms, and calculated statistical quantities such as the mean, standard deviation, skewness and kurtosis. Furthermore, we calculated the length of each branch using a on-line tool. Our results show the presence of 1) a deep seismic activity (33km) particularly in the WB, 2) a seismic crisis in 2005 in MER, 3) a migration of the seismic activity towards the south in the last ten years and 4) a trend for a shallower activity along the entire rift since 2010. We also find that the distinction between different branches further highlighted the dominant seismic activity in the MER and WB region which contrasted with the EB and SEB branches. Our findings have implications for the yield stress envelopes in the region and the correlation between the volcanic and seismic activity along the rift. They also suggest an influence of the sub-lithospheric flow of Afar mantle plume material on the seismicity along the rift.

Contents

List of Figures

List of Tables

List of Abbreviations

EARS: East African Rift System
EAR: East African Rift (or region)
WB: Western Branch
EB: Eastern Branch
MER: Main Ethiopian Rift
SEB: Southeastern Branch
E: East
W: West
N: North
S: South
USGS: United States Geological Survey
UTC: Coordinated Universal Time
DEM: Digital Elevation Model
QGIS: Geophysical Information System application

1 Introduction

An earthquake is a disturbance or vibration of the earth's surface caused by the abrupt release of seismic energy accumulated in underlying rocks within the earth [32].
Five large earthquakes together with one Tsunami in England that occurred between 1750 and 1755 prompted the beginning of modern seismology. This promoted an extensive study and cataloging of earthquakes based on their hypocenters, time of occurance and devastating effects. In recent years, the wide coverage of global communication network and improved sensitivity of seismic instruments have further enabled researchers to carry out more detailed analyse of the earthquake data.
Globally around 500 000 earthquakes occur annually with at least 100 000 being left significantly [3]. Many of those, 90%, are caused by tectonic movement while 10% results from volcanism, collapse of underground cavities, and human activities [26].

The concept of continental drift and sea floor spreading explains the formation of oceanic basins and oceanic crust within them. The oceanic crust is enclosed by continental formations. In other words, new oceanic basins or rift basins are the consequences of active divergence along continental margins or within the continents themselves [30].

Located on the African continental plate is the East African rift whose evidence was established by Suess (1891), following the explorations and discoveries of Livingstone, Stanley, Fischer, Thomson, Teleki and Von Hohnels during the 19^{th} century. In 1896, Gregory named it "the Great Rift Valley of East Africa", one of the most seismic area in the world, and in 1921 he described a system of graben basin including the Red sea and Dead sea systems, forming the Afro-Arabian rift system [30].

The earthquakes' frequent incident in East Africa give rise to the writings of many of the early explorers and travellers but the challenges of not having accurate maps in their researches resulted in the erroneous assessment of the seismicity within the region [14].
In 1906, Balladore reported isolated tremors in East Africa but attached no seismic importance to them in his map of the seismicity of Africa.
During 1921-1922, Krankel established the first positive correlation between the rift valleys and earthquake occurrence by collecting reports of felt earthquakes and producing a map indicating event frequencies. The seismic zone of Africa was described in a map produced by Sieburg (1932) who was the first researcher to indicate the activity of the Kavirondo Gulf as well as the other rift zones [14].

A summary of all previous reviews of seismicity of East Africa was published by Gorshkov in 1963; it showed not only a good correlation between obvious rift structures and earthquakes locations but also a wide spread of epicentre

locations in non rift areas [15].
Instrumental data was first used by both Gutenberg and Richter. Their work on East Africa listed events with magnitude range from 6.0 Mw to 7.7 Mw but the scarcity of stations used left the epicentral locations much in doubt [17].

Both Tobin et al. and Molnar and Aggarwal studied the macro-seismic activity associated with parts of the rift system within East Africa [28], [34]. Portable equipment located at many sites within East Africa was used for periods only exceeding a few days at any site. Through their conclusions, there was little or no activity, during the period of study, occurring outside the accepted rift valley structures and the activity was mainly concentrated within the Kavirondo Gulf rift and the eastern rift south of Lake Baringo with a relatively high level of activity around Lake Magadi in southern Kenya and northern Tanzania.

In 1979, Gouin worked on "Earthquake History of Ethiopia and the Horn of Africa" [16]; in his study, the earthquake history of the Ethiopian Western Plateau, Southeastern Plateau, Ethiopian Main Rift, Afar, the Southern Red Sea, Aden Western Sector, Gemu-Gofa and Turkana (Lake Rudolf) Rifts was developed.

Since the 1980s, the East Africa Rift System has remained the wide analogue to the early evolution's stage of passive continental margins preceding oceanic opening and an archetypal continental rift[6]. Many papers concern the various aspects of rift evolution [4], [7], [11], [27], [29], [33]. Furthermore, in the 1990s, the first reflection seismic profiling of rift basins in the region was also saw conducted. (e.g.,[10], [11], [25]).

The East African rift system shows up at the surface as a series of several thousand kilometers long aligned successions of adjacent individual tectonic basins (rift valleys), separated from each other by relative shoals and generally bordered by uplifted shoulders (See Figure 1). Each basin is controlled by faults and forms a subsiding graben or trough, near one hundred kilometers long, a few tens kilometers wide, empty or filled with sediments and/or volcanic rocks [6].
EARS is one of the major late Cenozoic active continental rifts in the world (together with Rio Grande, Baikal, Rhinegraben) with the following characteristics: high heat flow-predominantly basaltic and associated silicic volcanism (bimodal volcanism), lithospheric attenuation in both the crust and mantle, regional high elevation, low seismic velocity and high electrical conductivity, dominantly normal faulting in the crust with associated basin formation.

Previous studies of the seismicity in the East African region focused on local areas and the relation of the seismicity with the tectonics environment(e.g.[13], [24], [31],...). To our knowledge, however, no statistical study of the seismicity has been carried out at the scale of the entire region. This research aims at filling this gap.

Among the numerous questions that arise, those that this study proposes to address are:

1. What is the most likely magnitude of earthquakes in the region?
2. What does these magnitude suggest?
3. What is the most likely depth(s) of these earthquakes?
4. Are the depths suggesting different processes or are they similar?
5. Is there a migration of the seismicity along the rift (for example: from north to south, i.e. are the recent earthquakes more in the south compared to "old" earthquakes being further north)?
6. Where is most of the seismic activity? (i.e. where do you find most of the earthquakes?)
7. Is the seismicity similar between the different branches of the rift?
8. How does the seismicity of the East African rift compare with other rifts?

The next chapters are structured as follows:
In Chapter 2, we will present both how the seismicity record (data) to be used in this study was collected and the tools used for the statistical analysis.
In chapter 3, we will show the results of the analysis.
Finally, chapter 4 will broadly discuss the results.

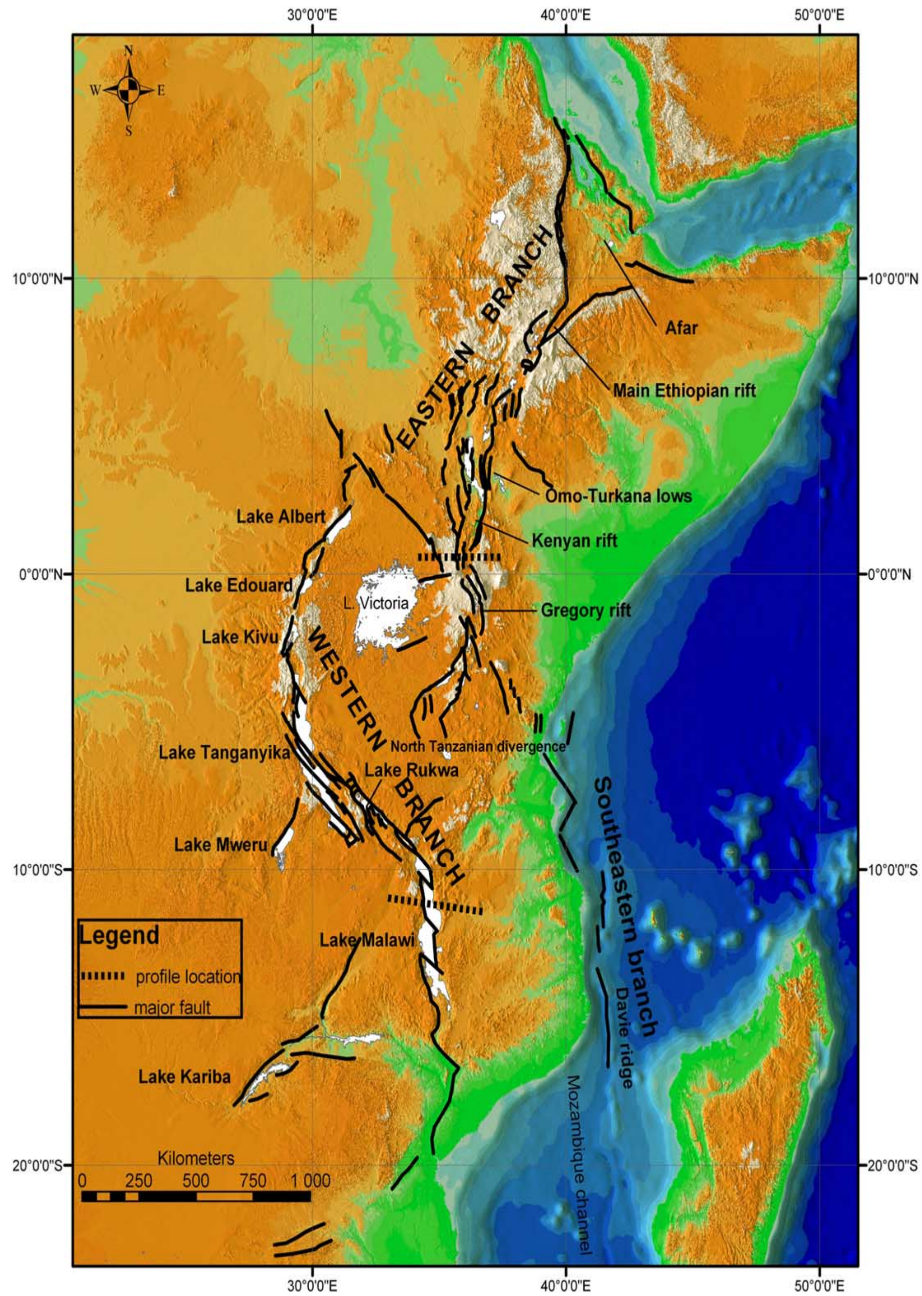

Figure 1: Hypsographic DEM of the East African rift system. Black lines: main faults; white surfaces: lakes; grey levels from dark (low elevations) to light (high elevations). From [6].

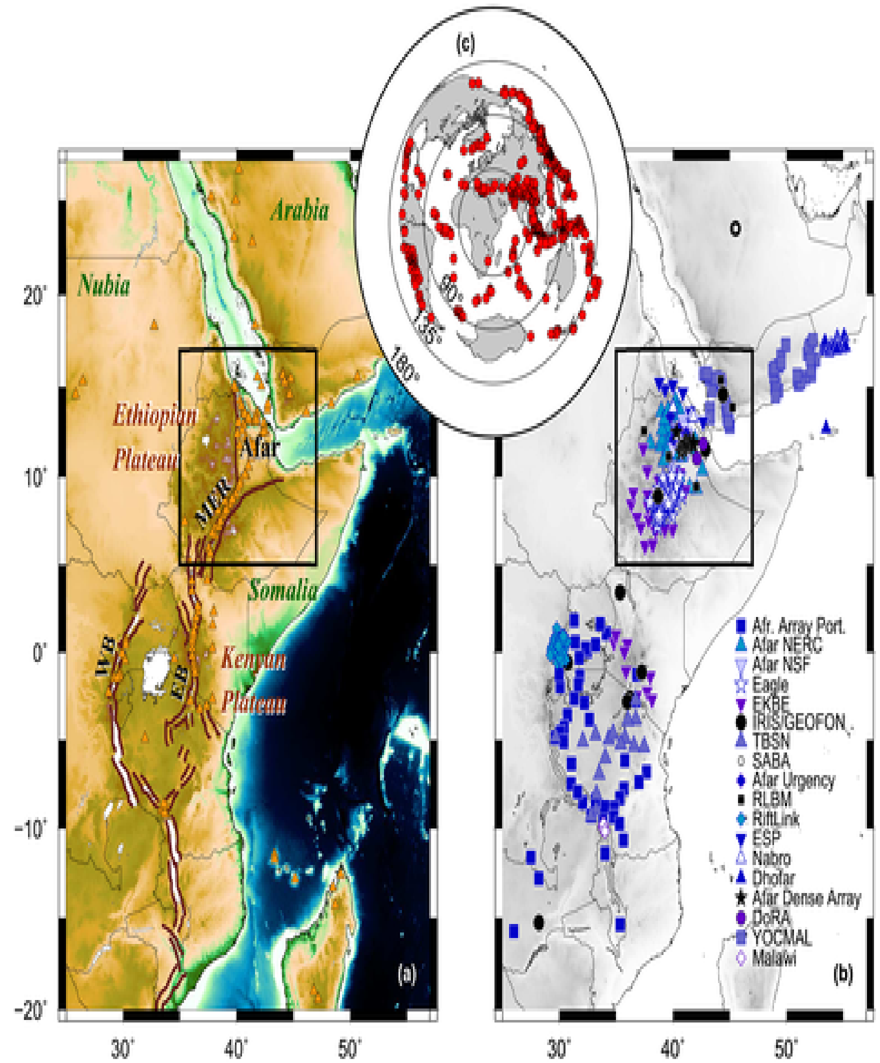

Figure 2: (a) Tectonic map of the EAR, showing the presence of two topographic domes, the main faults of the rift system (in brown), with the MER cutting through the Ethiopian plateau, the WB and EB around the Kenyan Plateau. The black rectangle indicates the area of study. (b) Distribution of all stations used. (c) Distribution of earthquake sources used for the S-SKS tomography. The circles show the source receiver distance from the center of black rectangle. From [8].

2 Methodology

Below we detail the origin of our data set and the method chosen for the analysis.

2.1 Seismicity record collection

We used the earthquake catalog available from the USGS website. In this catalog, the record of earthquakes in East Africa covers the entire period 1906-2020. Each record includes, among others, its magnitude, time, depth, latitude, longitude.

We collected data over the entire period and within the magnitude range [2, 10 Mw]. The region of the East African selected for the analysis was comprised between latitude 17.446^{o}S to 18.510^{o}N and longitude 28.389^{o}E to 43.506^{o}E as shown in Figure 3. Note that our data set does not include the seismic activity far to the west of the rift (e.g. in Republic Democratic of Congo).
According to USGS earthquake catalog, the first data in our region of interest, East African region, was recorded in Ethiopia on the 25th August 1906 at 13:47:26 (UTC) with magnitude 6.5 Mw, depth of 15.0 km and at Latitude 7.415^{o}N and Longitude 40.813^{o}E. Over the period of interest, magnitudes range from 2.0 to 10.0 Mw.

With the above criteria, we collected a record of 1983 earthquakes in the region, (see figure 3). We note that we did not apply any filter to the data of the catalog nor discriminated any potential outliers. We did not either extract the focal mechanisms as we did not focus our study on the link between seismicity and structural geology and tectonics.
We further distinguished different branches of the rift: the Eastern branch (EB), the Western branch (WB), the Main Ethiopian Rift (MER) and the Southeastern branch (SEB) (see figure 4).
Our definition of these different branches follows the majority of papers but mainly those of Chorowicz et al.[6] (see figure 1), Ebinger et al.[12] and Civiero et al.[8] (see figure 2).

2.2 Statistical analysis

Our analysis was statistical and it was performed using a home-made Python script. The manual of reference *matplotlib* served as a support during coding. We systematically analyzed the distribution of the seismicity as a function of time, depth, magnitude, latitude and longitude. We generated simple and bivariate histograms, mean, standard deviation, skewness and kurtosis. Furthermore, by using the *on-line tool* the length of each segment has been calculated (see Table 1). In the next section 3, we present the most relevant distributions.

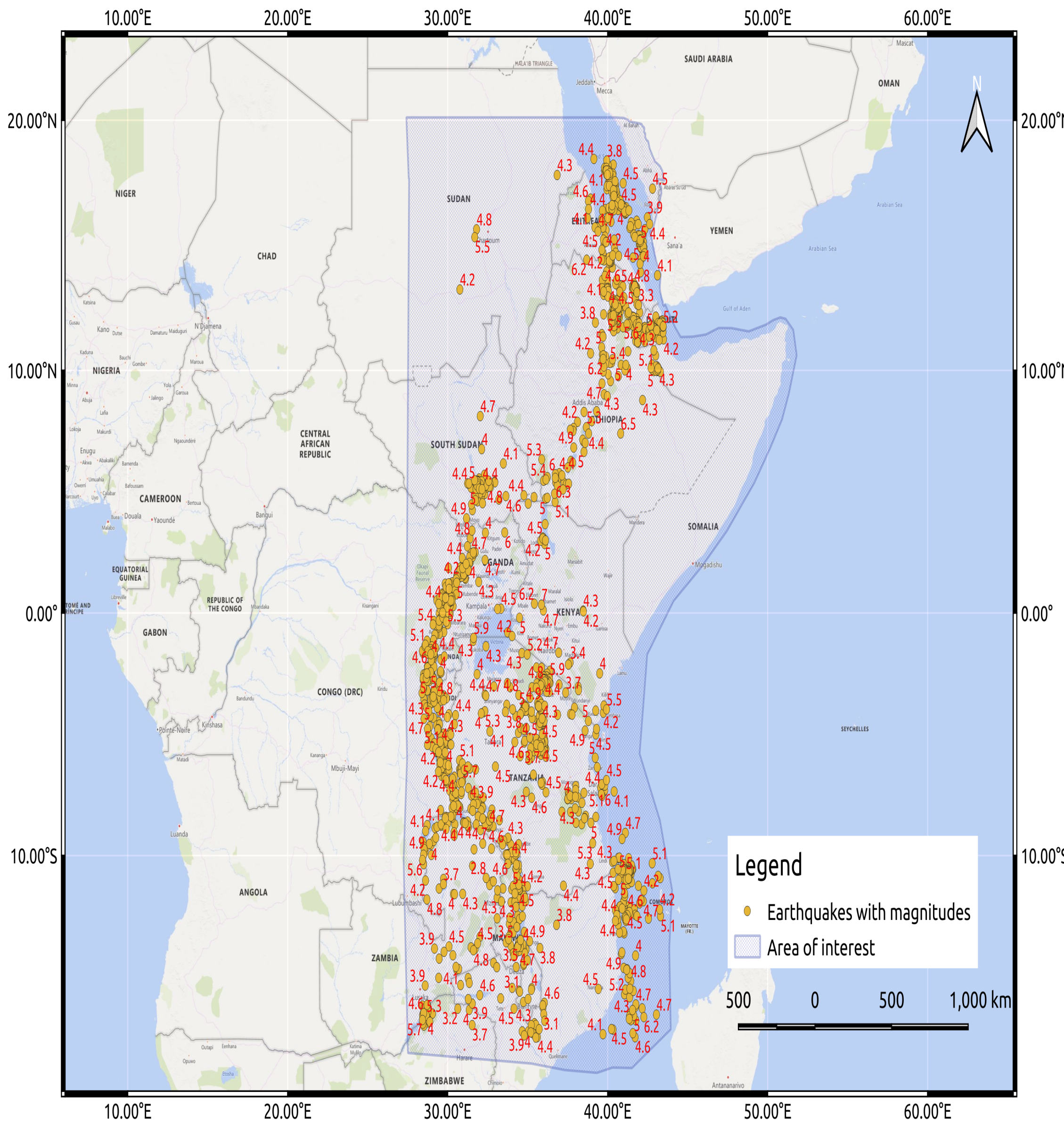

Figure 3: Seismicity in East African region (The map was done using QGIS).

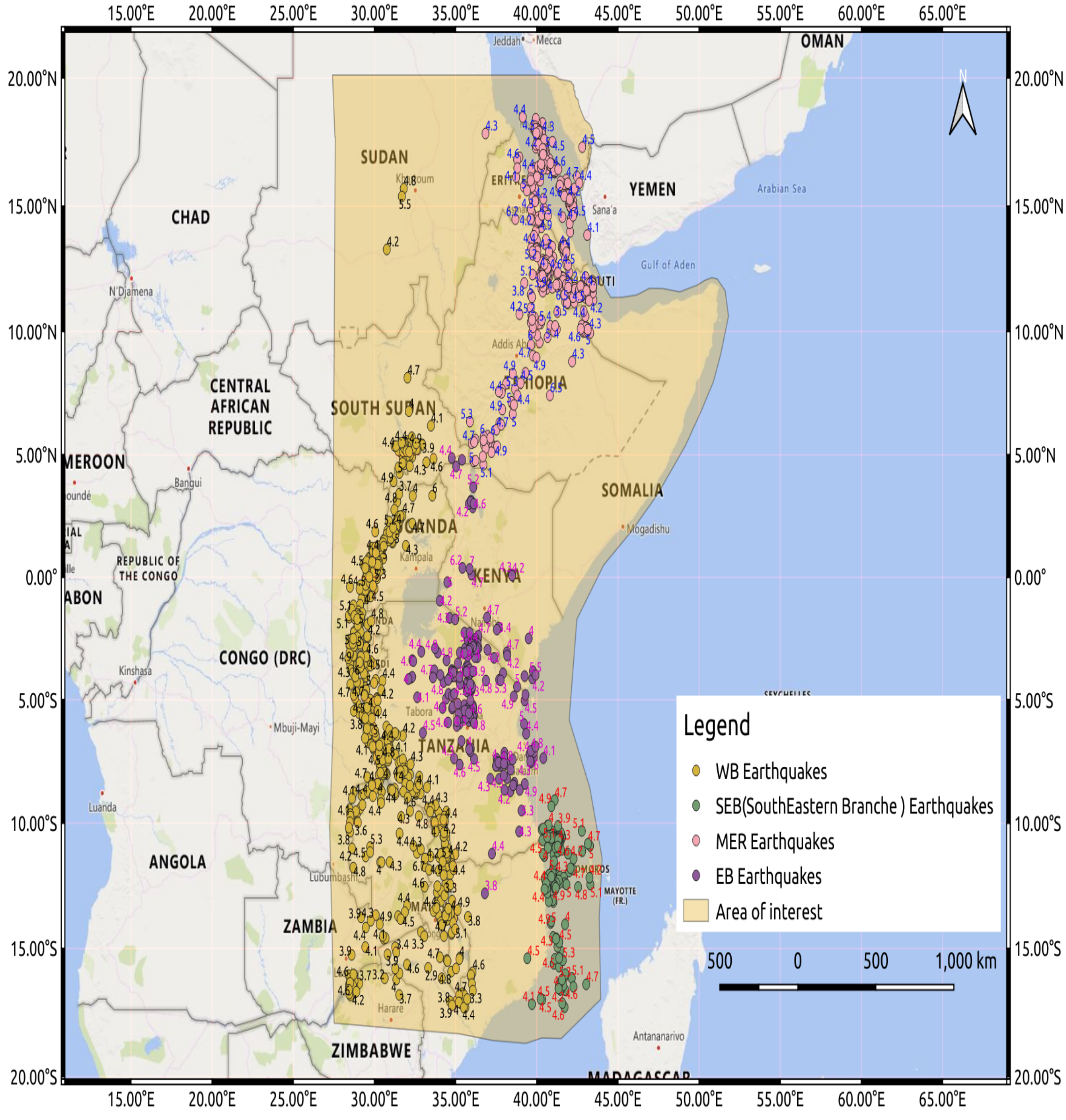

Figure 4: Distribution of the seismicity along the different branches: MER, EB, WB and SEB (The map was done using QGIS).

3 Results

3.1 Seismicity along the entire East Africa region

Figure 5 shows the histogram of the earthquakes' depth. The (discrete) distribution shows two remarkable depths, 10km with 1514 earthquakes and 33km with 203 earthquakes; the other remaining earthquakes are very shallow.

The distribution for the magnitude of earthquakes is shown in figure 6. It has its highest peak at magnitude 4.5 Mw with 196 earthquakes. The average magnitude of the earthquakes in East Africa is 4.57 Mw while the dispersion of the data-set relative to its mean (or Standard deviation) is 0.549 (or 54.9%) (see Table 1).

Figure 7 shows the earthquakes' time in East African region. The distribution has its highest peak is in 2005 with 202 earthquakes and 2007 with 131 earthquakes. There is not only a suggestion of a seismic crisis within and around this period range, 2005-2007, but there is also a slight trend for an increase of the earthquake activity since 1970. The latter trend, however, could reflect an increase of the seismic campaigns in the region rather than an intensification of the seismic activity.

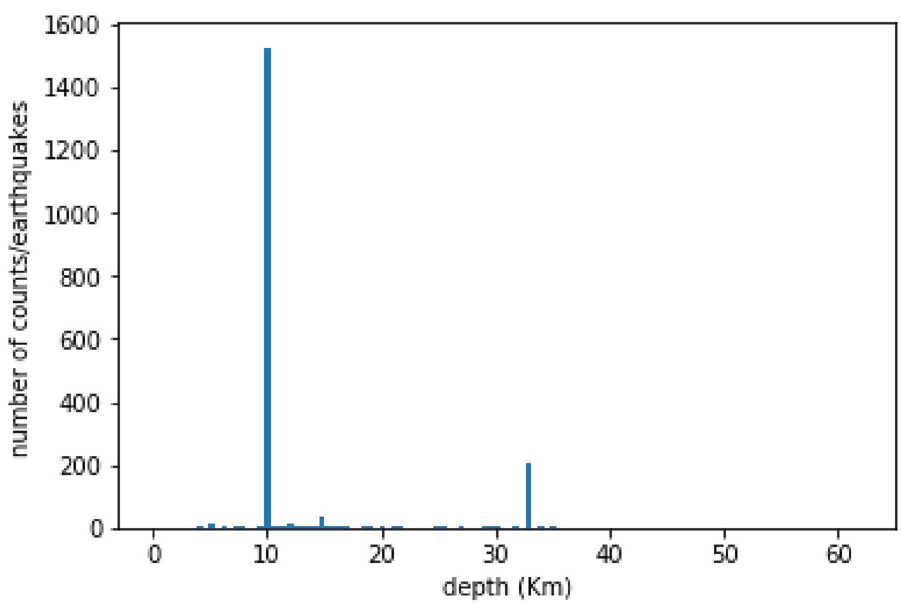

Figure 5: Depth of earthquakes in the entire East African region (116 bins were used to build the histogram, which represented a bin width of 0.534km).

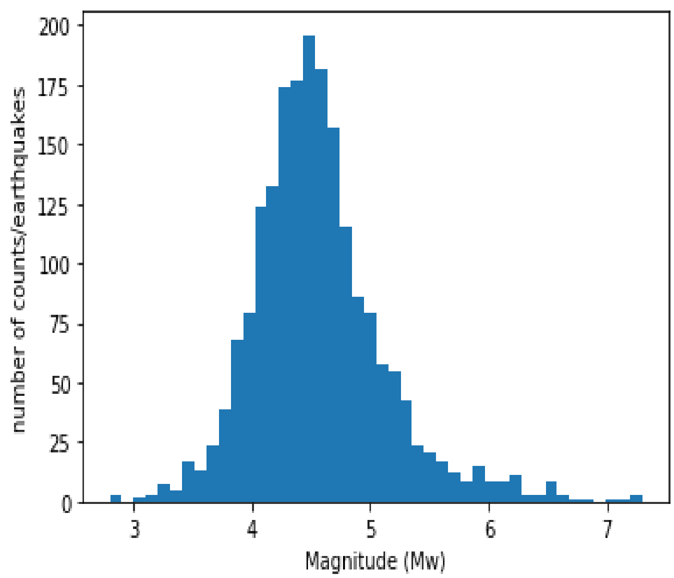

Figure 6: Magnitude of earthquakes in East African region (44 bins were used to build the histogram, which represented a bin width of 0.102 Mw).

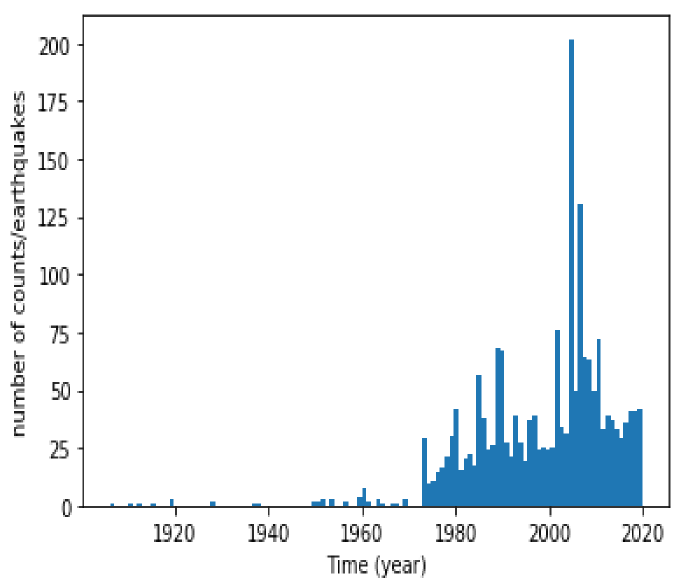

Figure 7: Time of earthquakes in East African region (116 bins were used to build the histogram, which represented a bin width of 0.983 year).

We further analysed some of the bivariate histogram to deeply understand well our region of interest:
In figure 8 which shows the relationship between earthquakes' time and magnitude, there is no big change in the distributions of magnitude between the two most intense seismic activity periods: around 2005 and 2018.
Figure 9 shows us the relationship between earthquakes' magnitude and their depth; it has two peaks in the magnitude range 4-6.5 Mw, one at 10 km and another at 33 km depth. The earthquakes which are out of this range are very shallow. There is no change in the magnitude of earthquake with the depth. So the distribution of the magnitude of earthquakes does not depend on depth or time. It is the same type of magnitude at all the depths of occurrence.
The relationship between earthquakes' depth and time are shown in figure 10 where the more recent activity is being shallower and the older one has been deeper.
From Figure 11, a big crisis in 2005 was in the northern region of the rift (In Afar, Ethiopia) [1]. There is both more activity in the southern region today and also a gap in the seismicity along the rift which region is between 6-11 degrees latitude.

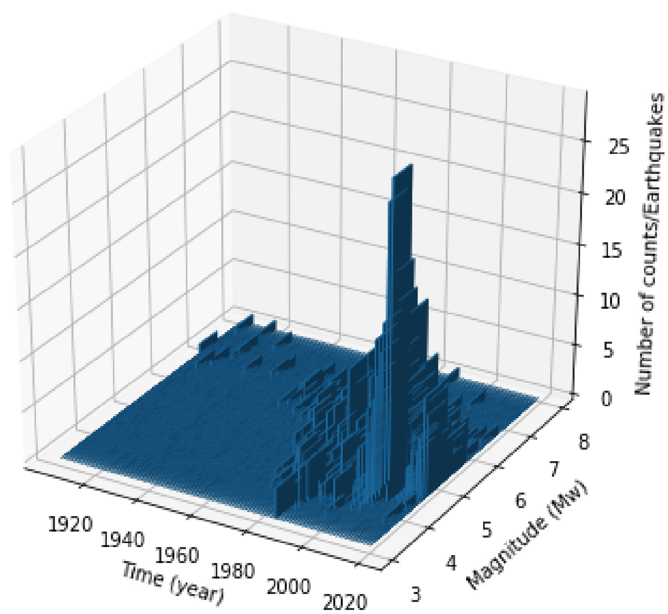

Figure 8: Bivariate histogram of earthquakes' time and their magnitude for the entire East African region. (116 and 44 bins were used on time and magnitude respectively).

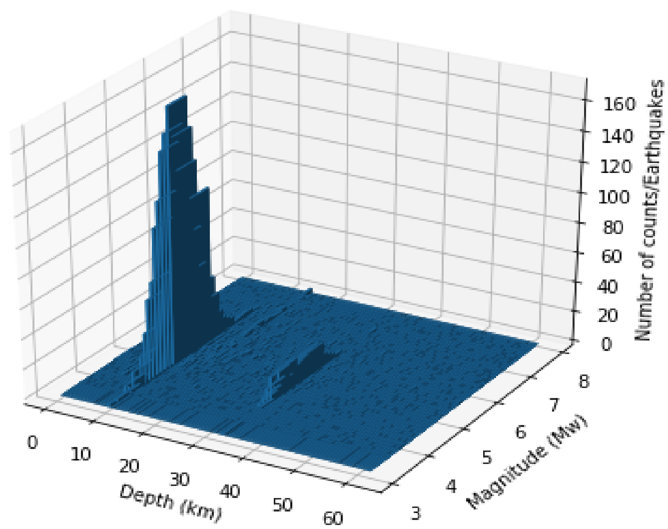

Figure 9: Bivariate histogram of earthquakes' depth and their magnitude for the entire East African region. (116 and 44 bins were used on depth and magnitude respectively).

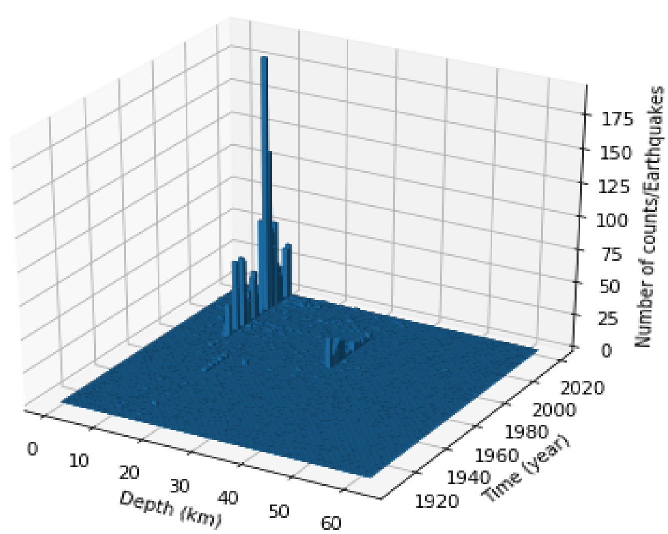

Figure 10: Bivariate histograme of earthquakes' time and their depth for the entire East African region. (116 bins were used on both the depth and time).

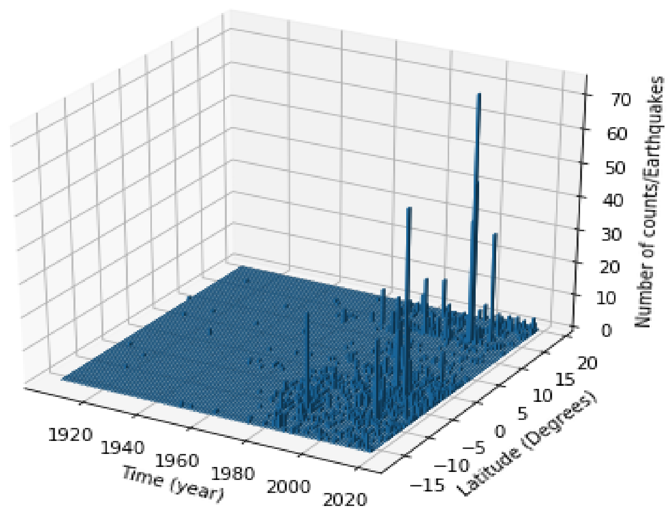

Figure 11: Bivariate histograme of earthquakes' time and their latitude for the entire East African region. (116 bins were used on both the time and latitude).

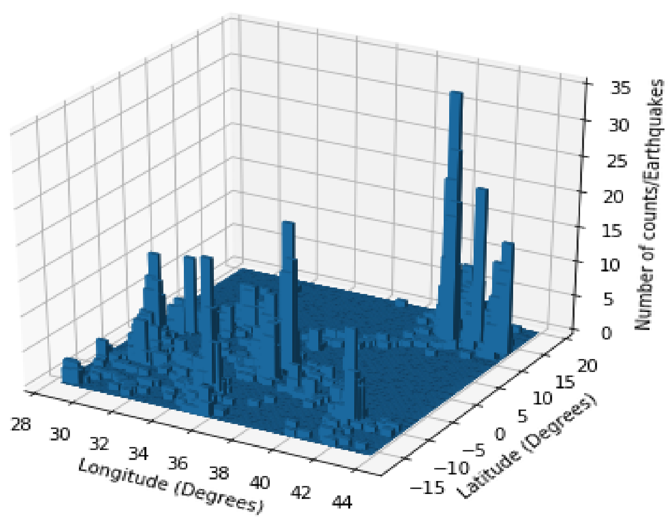

Figure 12: Bivariate histograme of earthquakes' longitude and latitude for the entire East African region. (116 bins were used on both the longitude and latitude).

The seismic activities are mostly in Western Branch at approximately 17.4^{o}S-6^{o}N of latitude and 28.3^o-35^{o}E with 788 earthquakes (39.7% of the total entire East African region events) and then in the Main Ethiopian Rift at 10^o-18^{o}N of latitude and 38^o-43.5^{o}E of longitude where there is 711 earthquakes (35.9% of the total entire East African region events) earthquakes (see Figure 12). The remaining, Eastern branch and Southeastern branch, have 17.2% and 7.2% respectively.

3.2 Seismicity in the Western branch (WB)

This branch runs from Lake Albert (Mobutu) in the north to Lake Malawi (Nyasa) in the south. It is made by several segments: the northern segment includes Lake Albert (Mobutu), Lake Edward and Lake Kivu basins, turning progressively in trend from NNE to N-S; the central segment trends NW-SE and includes the basins of lakes Tanganyika and Rukwa; the southern segment mainly corresponds to Lake Malawi and small basins more to the south [6].
In the western branch, the highest magnitude intensity took place in Lake Tanganyika region, Tanzania with magnitude 7.3 Mw, depth of 15 km, latitude 6.351^{o}S, longitude 31.27^{o}E on 13thDecember 1910 at 11:37:27 (time). (figure 14)
This is also the highest earthquake's magnitude recorded in East African region. Lake Tanganyika region in Tanzania hosted earthquakes with high magnitude in East Africa.

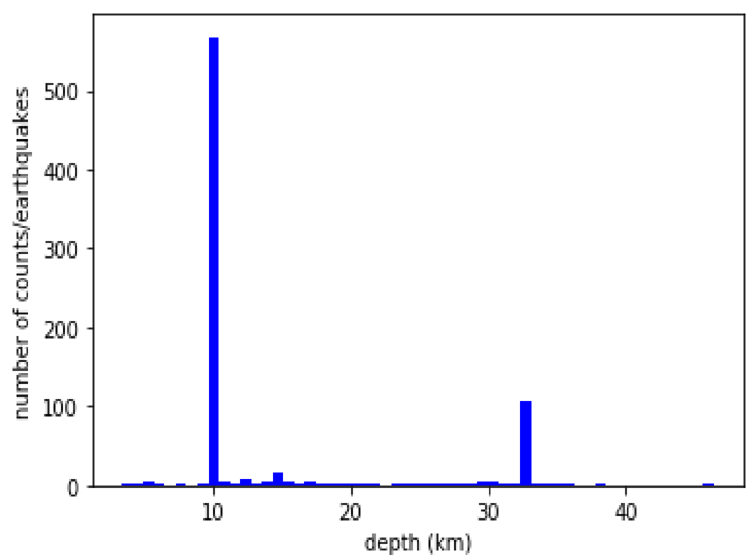

Figure 13: Depth of earthquakes in Western branch (bins=55).

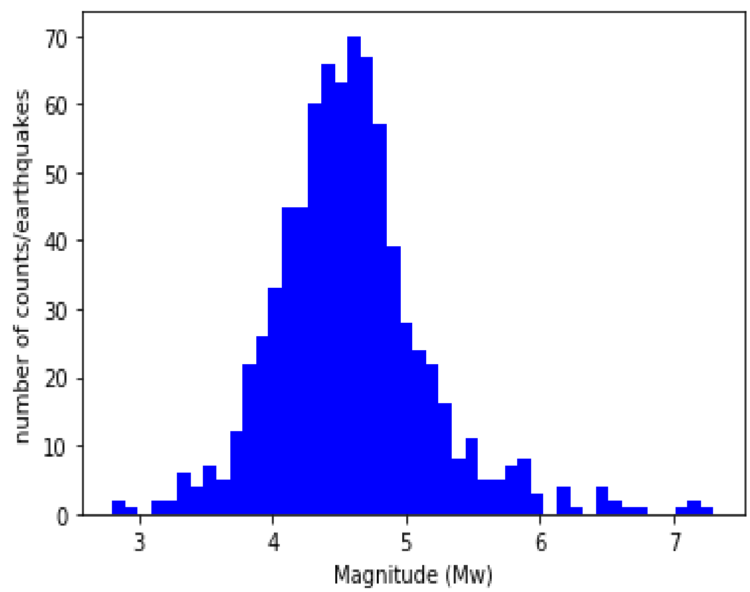

Figure 14: Magnitude of earthquakes in Western branch (bins=46).

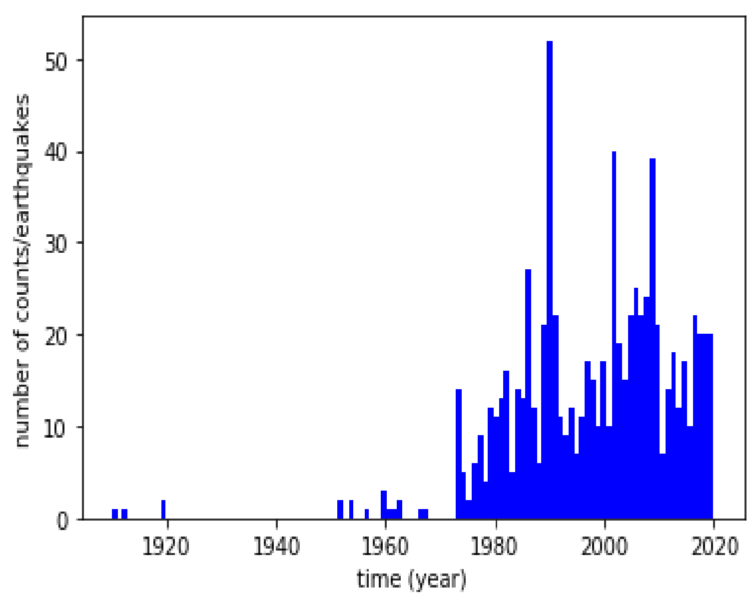

Figure 15: Time of earthquakes in Western branch (bins=112).

On the other hand, the lowest magnitude of earthquake in this branch (figure 14 is 2.8 Mw which took place in Zambia with depth 10 km, latitude 16.489^{o}S, longitude 16.489^{o}E on 28th March 1986. The deepest earthquake in this branch took place in Malawi with depth 46.4 km (see figure 13), latitude 13.791^{o}S, longitude 34.729^{o}E on 24th August 1998 at 12:12:09. While the shallowest earthquake recorded is 3.4 km (see figure 13) with magnitude 4.2 Mw, latitude 2.469^{o}S, longitude 29.593^{o}E on 8th April 2006, It took place in Rwanda.

The old earthquakes are the ones with the highest magnitude intensities.
The most likely magnitude of earthquakes in the Western branch is 4.6 Mw with 70 earthquakes (see figure 14), it is closer to the Western branch's magnitude average of 4.57 Mw.
The most frequently earthquake's depth in this branch is 10 km with 564 earthquakes (see figure 13). It is not so closer to mean depth of 14.4 km.
The highest number of earthquakes that were recorded per one year is 52 earthquakes in 1990. (see figure 15)

3.3 Eastern branch (EB)

The Eastern branch starts from the Omo-Turkana lows through Kenyan (Gregory) rifts and ends in the basins of the North-Tanzanian divergence in the south.

The highest magnitude intensity recorded in this branch took place in Kenya with magnitude 7.0 Mw (figure 17), depth of 15.0km, latitude 0.34^{o}N, longitude 35.86^{o}E on 6th January 1928 at 19:31:59. While the lowest recorded magnitude intensity took place at 28 Km S of Makueni, Kenya with magnitude 3.4 Mw (figure 17), depth 10 km, latitude 2.0577^{o}S, longitude 37.6557^{o}E on 8th August 2018 at 16:51:11.
The deepest recorded earthquake occurred at 33.8 km (figure 16) with magnitude 6.5 Mw. It took place in Tanzania at latitude 4.083^{o}S, longitude 35.243^{o}S on 7th May 1964 at 5:45:32. Also the shallowest recorded earthquake took place in Tanzania with depth 5 km (figure 16), magnitude 5.4 Mw, latitude 3.225^{o}S, longitude 35.744^{o}E on 15th May 1990 at 15:21:26.

The most frequently magnitude in this branch is 4.3 Mw with 41 earthquakes (figure 17) while the most likely depth is 10 km with 282 earthquakes (figure 16). The highest number of earthquakes recorded per one year is 91 earthquakes in 2007 (figure 18).

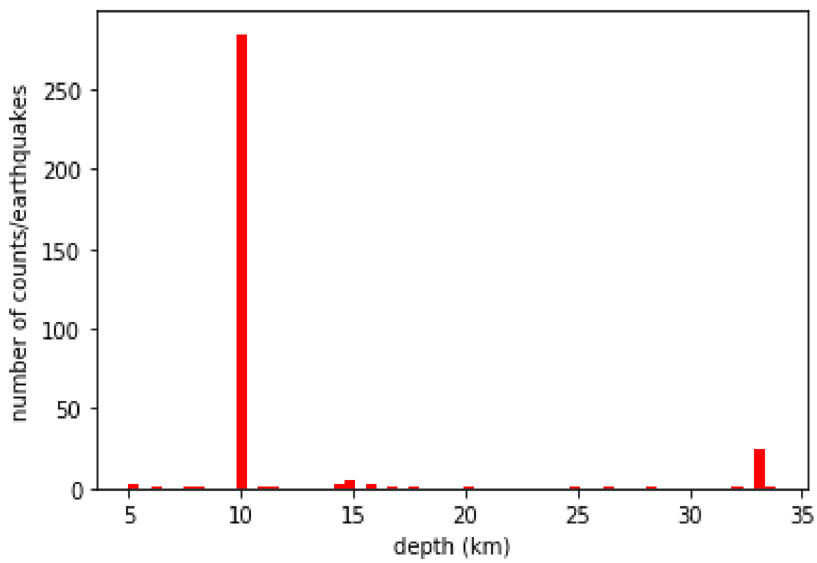

Figure 16: Depth of earthquakes in Eastern branch (bins=60).

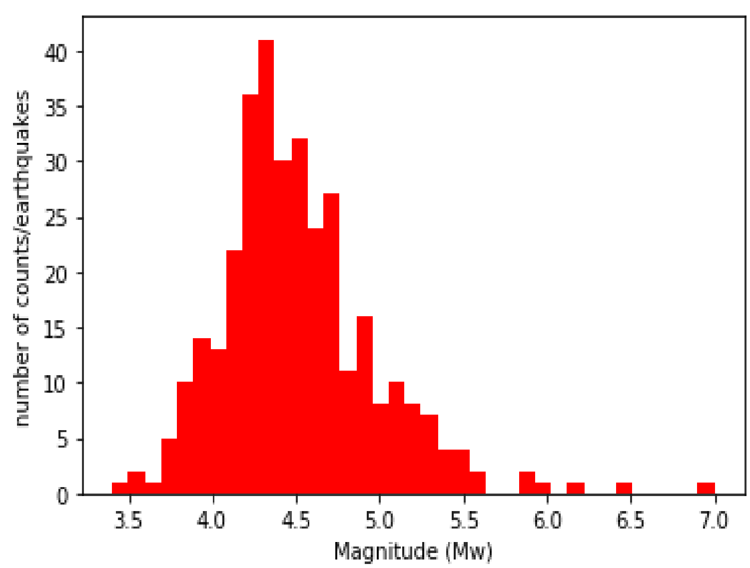

Figure 17: Magnitude of earthquakes in Eastern branch (bins=37).

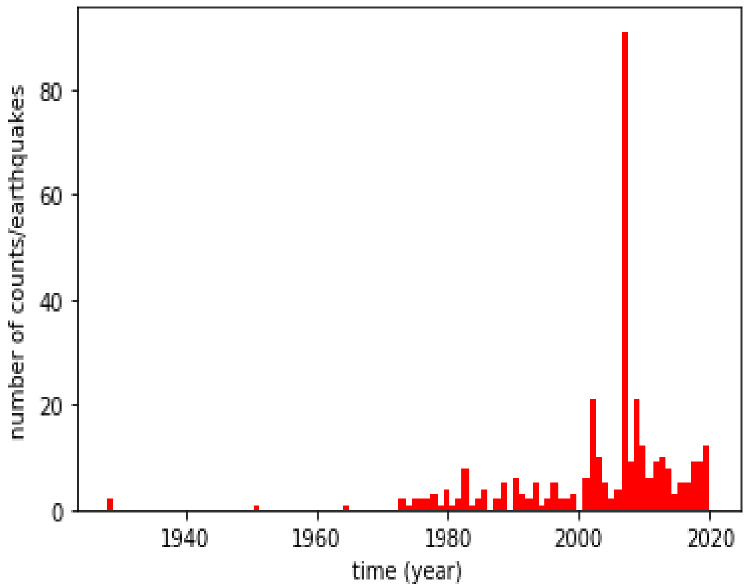

Figure 18: Time of earthquake in Eastern branch (bins=95).

3.4 Main Ethiopian rift (MER)

In this study the Main Ethiopian rift combines both the Afar triangle from its north and the Ethiopian rift which ends in the north of Omo-Turkana lows.
The seismicity along the Ethiopian rift and in the Afar region has been studied extensively ([2], [19], [21], [22]). According to the USGS earthquake catalog, the first recorded earthquake in East Africa on 25^{th} August 1906 at 13:47:26 with magnitude 6.5 Mw, depth 15 km, latitude 7.415^{o}N and longitude 40.813^{o}E was found in MER precisely in Ethiopia.
The recorded earthquake with the highest magnitude intensity took place in the Red sea with magnitude 6.6 Mw (figure 20), depth 33 km, latitude 16.659^{o}N, longitude 40.278^{o}E on 28^{th} December 1977 at 02:45:36 while the lowest recorded magnitude is 3.2 Mw (figure 20) which took place in Golfe de Tadjoura, Djibouti with depth 7.5 km, latitude 11.742^{o}N, longitude 43.145^{o}E on 12^{th} January 2000 at 02:20:38.
On the other side, the deepest recorded earthquake also took place in Golfe de Tadjoura, Djibouti with depth 62 km (figure 19), magnitude 4.9 Mw, Latitude 11.555^{o}N, longitude 42.572^{o}E on 8^{th} November 1978 at 05:08:01 while the lowest earthquake's depth is 0.1 km (figure 19) which took place in Ethiopia with magnitude 4.2 Mw, latitude 12.045^{o}N, longitude 40.413^{o}E on 22^{nd} September 2005 at 12:10:38.

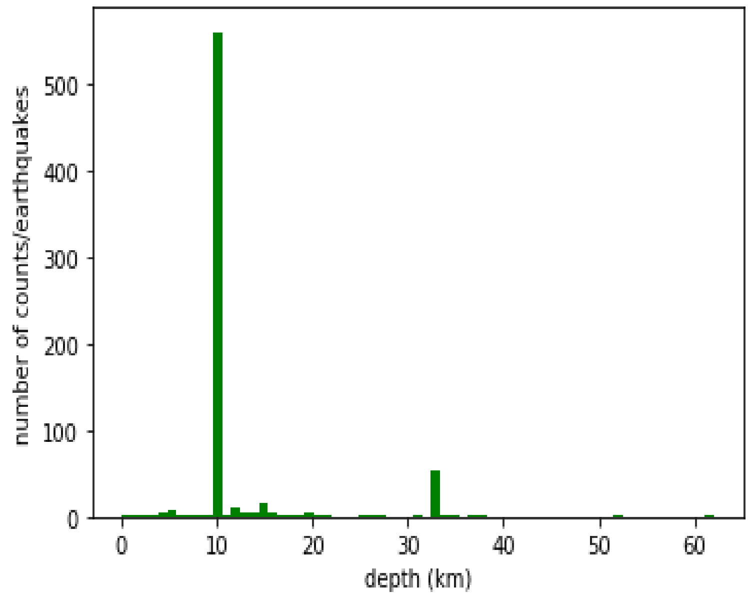

Figure 19: Depth of earthquakes in MER (bins=65).

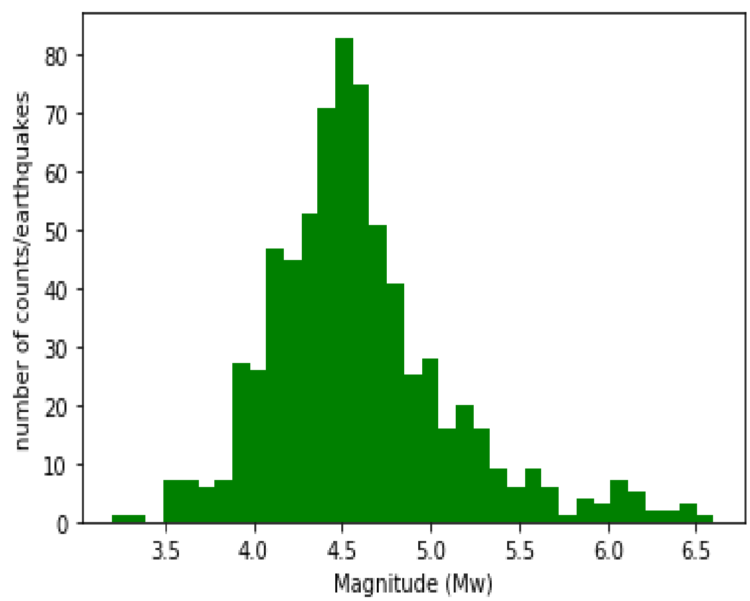

Figure 20: Magnitude of earthquakes in MER (bins=35).

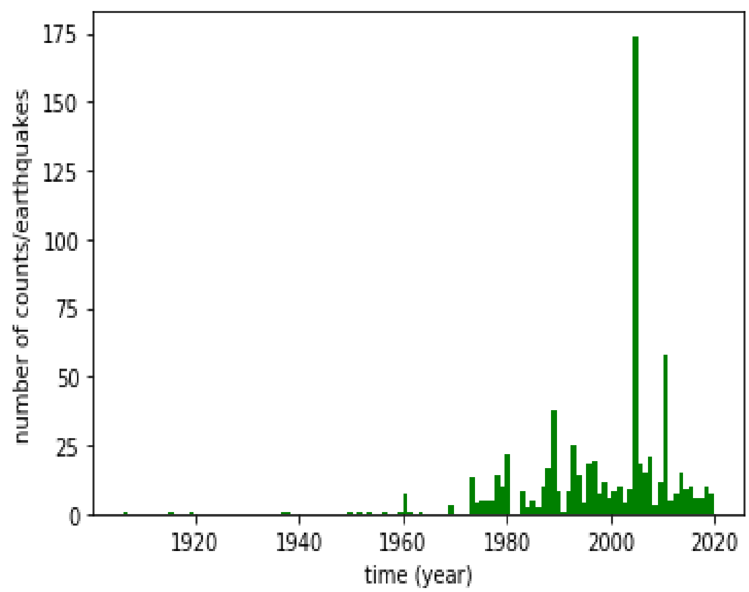

Figure 21: Time of earthquakes in MER (bins=116).

Since 2009, all recorded earthquakes have magnitude greater than four (4.0 Mw) while since 2001, earthquakes are shallower with depth less than 22 km except only one having depth 27.5 km with magnitude 3.7 Mw that took place in Ethiopia on 11^{th} July 2005 at 20:36:11.

The most likely magnitude of earthquakes in this region is 4.5 Mw, with 83 earthquakes (figure 20), which is really closer to the earthquakes' magnitude mean average of 4.589 Mw.
The most frequent depth of earthquakes is 10 km with 551 earthquakes (figure 19) which is somehow closer to the depth's mean average of 12.43 km.
The highest number of earthquakes recorded in one year is 174 in 2005 (figure 21).

3.5 Southeastern branch (SEB)

In this branch, the highest earthquake's magnitude intensity recorded is 6.4 Mw (figure 23), It took place in Comoros region with depth 10 km, latitude 10.562^oS, longitude 41.424^oE on 14^{th} May 1985 at 18:11:08 while the lowest recorded magnitude intensity is 3.5 Mw (figure 23) with depth 10km, latitude 13.135^oS, longitude 40.74^oE, it took place in Mozambique.

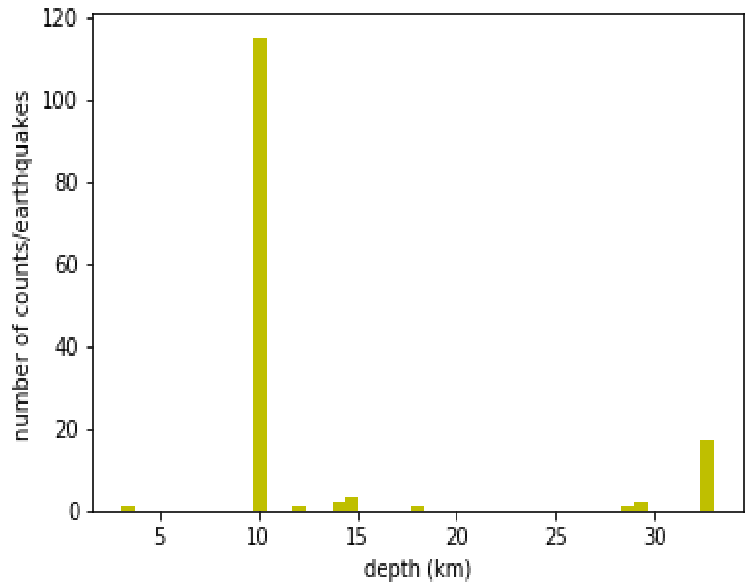

Figure 22: Depth of earthquakes in Southeastern branch (bins=45).

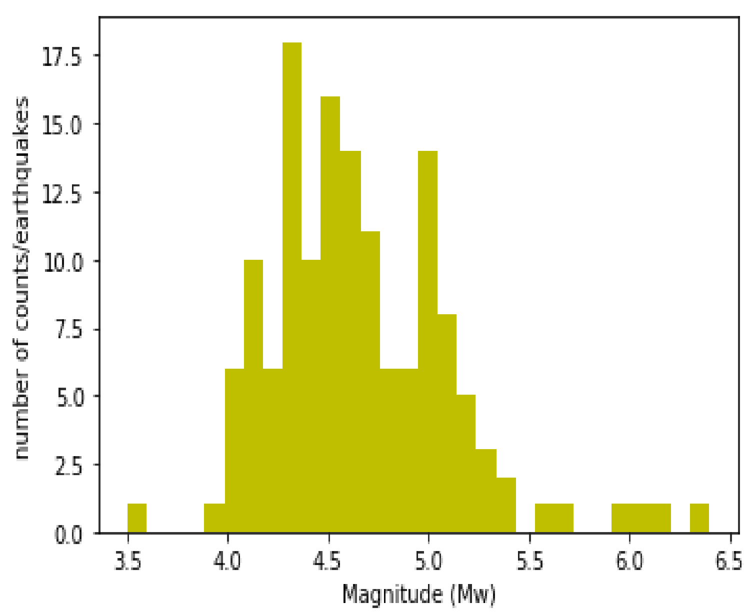

Figure 23: Magnitude of earthquakes in Southeastern branch (bins=30).

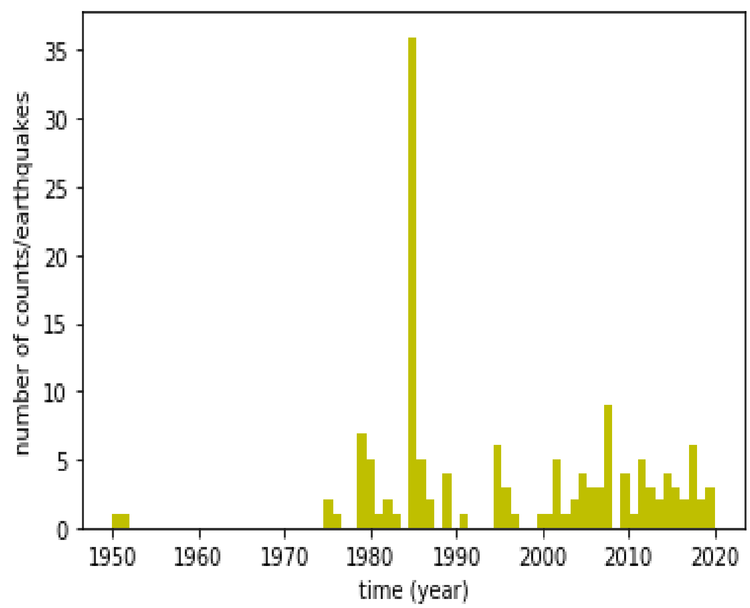

Figure 24: Time of earthquakes in Southeastern branch (bins=71).

The deepest earthquake in this branch occurred at 33 km (figure 22). This depth was recorded for 17 earthquakes in different parts in this branch. On the other side, the shallowest recorded earthquake took place in Comoros region with depth 3.1 km (figure 22), magnitude 5.0 Mw, latitude 11.812^{o}S, longitude 42.082^{o}E, on 16th September 2007 at 14:01:47.

The most frequent earthquakes' magnitude in this branch is 4.3 Mw with 18 earthquakes (figure 23) while the most frequently depth is 10 km with 115 earthquakes (figure 22). The highest number of earthquakes recorded during one year is 36 earthquakes in 1985 (figure 24).

3.6 Comparison between branches

To summarise this section let's now analyse figures 25, 26 and 27 which show the comparison of magnitude, depth and time respectively across the different branches.
In figure 26, there is almost no difference in magnitude between the different branches. The seismicity activity in WB and MER are almost the same. The only slight difference in magnitude along SEB and EB compared to other branches may indicate changes in the local extensional stresses.
The highest number of earthquakes are in the Western branch with 40% while the Southeastern branch is the one with few number, 7%, compared to other branches in East Africa (See Table 1).

Figure 25 shows that the Main Ethiopian rift has both the deepest (in Golfe de Tadjoura, Djibouti) and the shallowest (in Ethiopia) earthquakes with 62 km and 0.1 km respectively.
At 10 km depth, the Western branch is the one with the highest number of earthquakes, 564, while the Southeastern branch has the lowest number of earthquakes, 115. Similarly at 33 km depth, Western branch has a higher number with 106 earthquakes while Southeastern branch has a lower number with 17 earthquakes. Other depths are very shallow.
Figure 27 shows a seismic crisis in 2005 located at MER that has been almost synchronous to an increase of the seismic activity in the EB. The seismic activity has greatly subsided in MER since 2010 while the seismic activity is predominant along the Western branch.

Object	**EAR**	**WB**	**MER**	**EB**	**SEB**
Mean	4.572516	4.575635	4.589311	4.494910	4.648951
St.dev	0.549172	0.597934	0.534551	0.480682	0.467668
Skew	0.941871	0.857866	1.136090	0.972025	0.968087
Kurt	2.412985	2.588117	1.674764	3.032211	1.817047
Events	1983	40%	36%	7%	17%
Length (km)	4326	4045	1787	2009	1220
Events/Length	0.458	0.196	0.399	0.169	0.114

Table 1: Mean, Standard deviation, Skewness and Kurtosis of earthquakes' magnitude in East Africa region, Western branch (WB), Eastern branch (EB), Main Ethiopian rift (MER) and Southeastern branch (SEB). The number of events, length and events/length of both the entire EAR and each branch are also given.

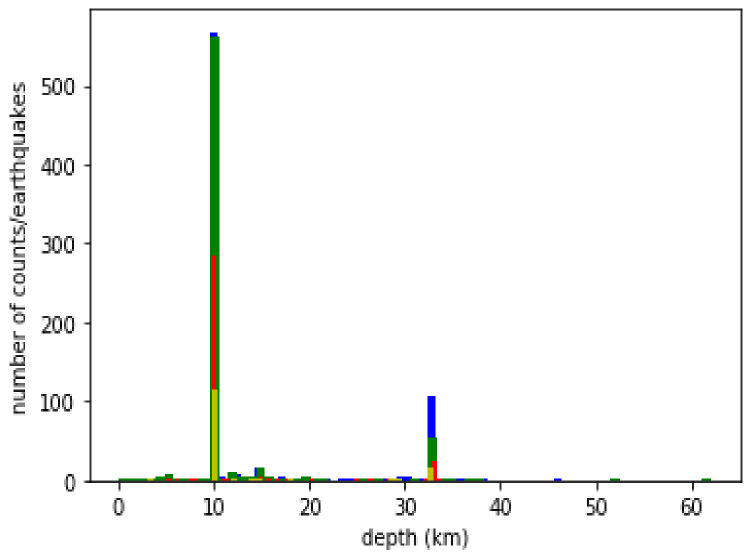

Figure 25: Comparison of earthquakes' depth and their counts in all branches: EB(in red), WB(in blue), MER(in green), SEB(in yellow)

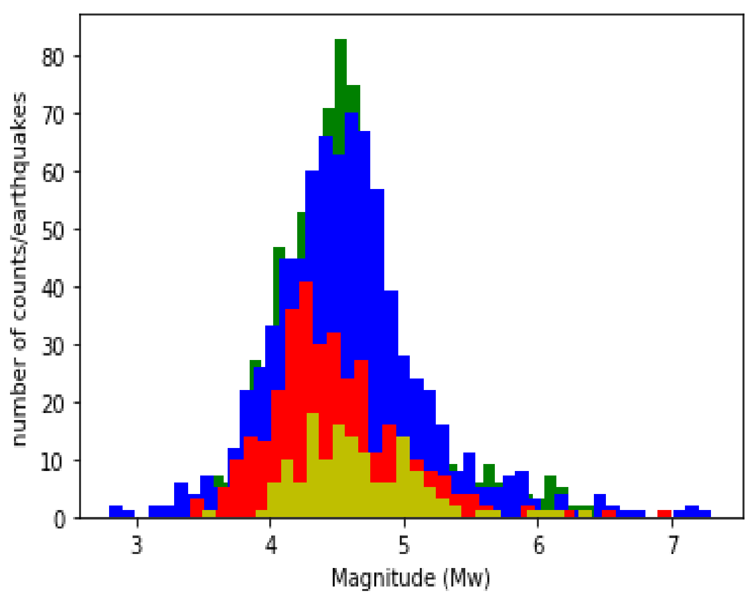

Figure 26: Comparison of earthquakes' magnitude and their counts in all branches: EB(in red), WB(in blue), MER(in green), SEB(in yellow)

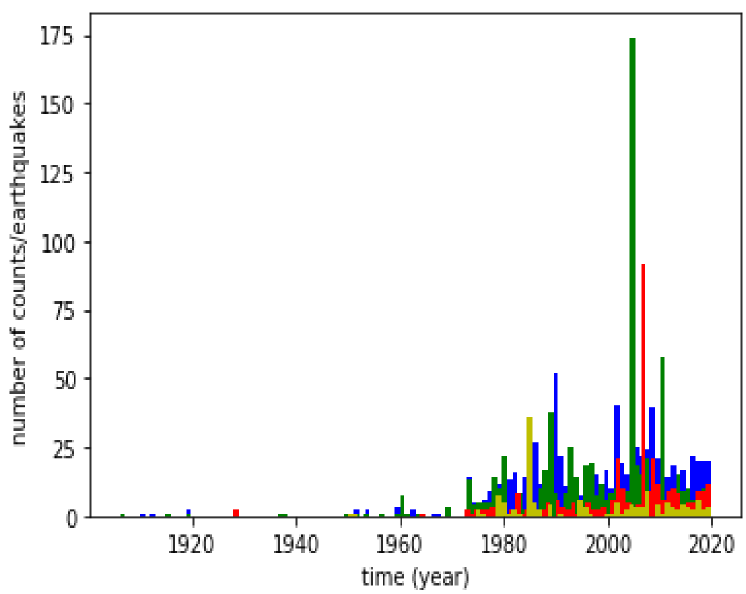

Figure 27: Comparison of earthquakes' time and their counts in all branches: EB(in red), WB(in blue), MER(in green), SEB(in yellow)

4 Discussion and Conclusion

In this study, we looked at the seismicity of the East African Rift using a statistical approach. Unlike most localised studies (e.g.[6],[12], [14], [28], [34]), we considered the seismicity along the entire length of the rift allowing us to have a global view of the seismic activity. Our record of 1983 seismic events was extracted from the USGS catalogue with events spanning the period 1906-2020.

The most likely magnitude for earthquakes in the region is 4.57 Mw as shown, for instance, in Figure 6 and Table 1. There is almost no differences between the different branches of the rift in terms of magnitude. In particular the seismicity activity of MER and WB are almost indistinguishable with respect to magnitude. The averaged magnitude is typical of regions where the tectonic setting is extension such as in a rift, where plate divergence occurs. By comparison, convergent zones such as subduction zones have typically earthquakes of higher magnitude. The slight differences in the magnitude along SEB and EB compared to MER and WB may indicate changes in the local extensional stresses.

We found two characteristics depths for earthquakes along the entire rift at 10 km and 33 km (see Figure 5). Although the same trend is found in the different branches, the Western Branch distinguishes itself by having the most occurrences at 33 km without a change in magnitude as shown in Figure 9 and 25. The presence of earthquakes at a depth of 33 km, where the crust should be ductile and therefore prohibit brittle failure is still not well understood in rifting regions. One proposed hypothesis is that extensional forces linked to rift dynamics could result in a deeper brittle–ductile transition [5]. This explanation however ignores the presence of mantle plume material beneath the rift as is the case in the EAR, which originates from the Afar deep mantle plume [36].

The seismic activity along the entire rift is predominantly in MER and WB. In terms of number of earthquakes, the Western branch accounts for 40% of the total number of events, MER for 36%, where SEB and EB account for 17% and 7% respectively. Now, the number of events along each branch relative to the segment's length (number of events/branch length) is 0.196 event km^{-1}, 0.399 event km^{-1}, 0.168 event km^{-1} and 0.114 event km^{-1} in WB, MER, EB and SEB respectively (see Table 1). So, the activity is dominant in MER followed by WB, EB and SEB. We note however that the difference in seismicity activity between the two branches, WB and EB, is only 14% which is not significant.

Our analysis of the earthquake activity over the period 1906-2020 shows that the most recent activity is actually shallow (10 km) whereas deep earthquakes occurred in the early 2000. Such events are curiously absent today (see Figure 10). We found a noticeable seismic crisis around 2005 that affected MER and all branches except (SEB) (see Figures 15, 18, 21 and 24). In Afar, the later crisis was associated with a volcanic crisis as described by Ayele et al. [1], but eruptions and dyke intrusions further south did not appear to be reported. In the last 10 years, the seismic activity appears to have migrated towards the southern part of the rift and especially along its Western branch (see Figure 11). This migration could indicate a magma pathway and southward uppermost-mantle flow of the Afar plume material, a trend that would coincide with the general southward motion of the Afar mantle plume proposed by Hassan et al. [18].

In this study, we have observed lower crustal seismicity (33 km). This is actually observed in other continental rift zones (e.g. Baikal) [9]. Yet, the EAR seems to have a seismic signature on its own. For instance, in Baikal continental rift zone almost all depths are more continuous (see Figure (3) of [9]) whereas in our case, East African rift, we have two peaks at 10 km and 33 km depth with almost nothing in between (See Figures 5 and 9) ([9], [35]). Now, the EAR is associated with the Afar plume and more broadly with the African super-plume (see for instance Figure 1 of Koptev et al. [23]). In the case of the Baikal and Rio Grande, a mantle plume has also been invoked in the rifting (e.g. Zhao et al. [37]) but the presence of a deep mantle plume is not as clear cut. We should thus expect a distinct magma-driven seismicity in these three rifts.

A correlation between the volcanic and seismic activity along the EAR has been exemplified during the Afar crisis [1] or the Magadi-Natron-Manyara section of the East African Rift [29]. Magma-propagation-driven thus appears to contribute to the seismicity along the rift. Yet, such a correlation is still questionable along the West branch. Koptev et al [23] refers to the West branch as "a magma-poor (western) branch". By contrast, Jakovlev et al [20] found a low-velocity zone indicative of a reservoir of magma along the Northern part of the Western Branch, which they related to earthquake swarms at depths between 5 and 16 km.

To conclude, this study allowed to have a global view the seismicity along the East African Rift and its evolution since 1906. It showed the presence of deep seismic activity (33 km) particularly in the WB, a seismic crisis in 2005 in MER, and the migration of the seismic activity towards the south in the last ten years. The distinction between the different branches further highlighted the dominant seismic activity in the MER and WB region which contrasted with the EB and SEB branches. The seismic activity at 33 km depth (in a priori non-brittle region) seen principally in the WB branch and to a lesser degree in MER is an interesting feature, especially as we did not identify any change in the distribution of the earthquake magnitude with depth. This finding could be investigated further in the future by relating the earthquakes/depth histograms with yield-stress envelopes (YSEs). The southward migration of a shallower seismicity and its connection with magma propagation along the rift in the last ten years would also deserve more analysis.

5 Acknowledgement

First of all, I express my deepest gratitude to my supervisor **Dr. Catherine Meriaux**, from the School of Earth, Atmosphere and Environment, Monash University, Australia and the East African Institute for Fundamental Research (ICTP-EAIFR), University of Rwanda, Rwanda for her valuable continuous support, time, explanation, encouragement and guidance. Without her this work would not be achieved. I hope this good collaboration will be continued even after this Thesis.

I deeply express my gratitude to both **Dr. Omololu Akin Ojo**, Director of ICTP-EAIFR, for his higly valuable academic and financial helps and support during my Master studies and the financial support from the Government of Rwanda through High Education Council - Ministry of Education.

I also express my gratitude to all ICTP-EAIFR-Rwanda staff together with both ICTP-EAIFR-Rwanda and ICTP-TRIESTE-Italy lectures who contributed a lot in my Masters studies.

Finally, I deeply express my highest gratitude to my lovely future wife "**Santa Kevine UMUTONIWASE**", my lovely family (Father, Mother and Brothers), my colleagues and friends for all their help and supports.

6 AppendixA

6.1 PYTHON SCRIPT

This script contains all codes used to produce different outputs which helped us to analyse well statistically the seismicity in East African region

Importing toolboxes

```
from mpl_toolkits import mplot3d
import pandas as pd
import seaborn as sns
import matplotlib.pyplot as plt
import matplotlib.cm as cm
from mpl_toolkits.mplot3d import Axes3D
import numpy as np
import statistics as stats
from scipy.stats import kurtosis, skew
```

Reading data of the entire EAR

```
data = pd.read_csv('querydata.csv', encoding = 'utf-8').fillna(0)
```

Reading data of the WB, EB, MER and SEB respectively

```
dataWB= pd.read_csv('queryWRVdataNew.csv', encoding = 'utf-8').
    fillna(0)
dataEB= pd.read_csv('queryERVNewNewdata.csv', encoding = 'utf-8').
    fillna(0)
dataMER= pd.read_csv('queryMERdata.csv', encoding = 'utf-8').fillna
    (0)
dataSEB= pd.read_csv('querySERV.csv', encoding = 'utf-8').fillna(0)
```

PLOTTING DIFFERENT HISTOGRAMS

Histograms of the entire EAR

```
plt.xlabel('depth (Km)')
plt.ylabel('number of counts/earthquakes')
plt.title("Histogram of Earthquakes' depth in Entire EAR")
plt.hist(data.depth, bins=116)
```

```
plt.xlabel('Magnitude (Mw)')
plt.ylabel('number of counts/earthquakes')
plt.title("Histogram of Earthquakes' Magnitude in entire EAR")
plt.hist(data.mag, bins=44)
```

```
plt.xlabel('Time (year)')
plt.ylabel('number of counts/earthquakes')
plt.title("Histogram of Earthquakes' time in entire EAR")
plt.hist(data.time, bins=116)
```

Histograms of the WB

```
plt.xlabel('depth (Km)')
plt.ylabel('number of counts/earthquakes')
plt.title("Histogram of Earthquakes' depth in WB")
plt.hist(dataWB.depth, bins=55)
```

```
plt.xlabel('Magnitude (Mw)')
plt.ylabel('number of counts/earthquakes')
plt.title("Histogram of Earthquakes' Magnitude in WB")
plt.hist(dataWB.mag, bins=46)
```

```
plt.xlabel('Time (year)')
plt.ylabel('number of counts/earthquakes')
plt.title("Histogram of Earthquakes' time in WB")
plt.hist(dataWB.time, bins=112)
```

Histograms of the EB

```
plt.xlabel('depth (Km)')
plt.ylabel('number of counts/earthquakes')
plt.title("Histogram of Earthquakes' depth in EB")
plt.hist(dataEB.depth, bins=60)
```

```
plt.xlabel('Magnitude (Mw)')
plt.ylabel('number of counts/earthquakes')
plt.title("Histogram of Earthquakes' Magnitude in EB")
plt.hist(dataEB.mag, bins=37)
```

```
plt.xlabel('Time (year)')
plt.ylabel('number of counts/earthquakes')
plt.title("Histogram of Earthquakes' time in EB")
plt.hist(dataEB.time, bins=95)
```

Histograms of the MER

```
plt.xlabel('depth (Km)')
plt.ylabel('number of counts/earthquakes')
plt.title("Histogram of Earthquakes' depth in MER")
plt.hist(dataMER.depth, bins=65)
```

```
plt.xlabel('Magnitude (Mw)')
plt.ylabel('number of counts/earthquakes')
plt.title("Histogram of Earthquakes' Magnitude in MER")
plt.hist(dataMER.mag, bins=35)
```

```
plt.xlabel('Time (year)')
plt.ylabel('number of counts/earthquakes')
plt.title("Histogram of Earthquakes' time in MER")
plt.hist(dataMER.time, bins=116)
```

Histograms of the SEB

```
plt.xlabel('depth (Km)')
plt.ylabel('number of counts/earthquakes')
plt.title("Histogram of Earthquakes' depth in SEB")
plt.hist(dataSEB.depth, bins=45)
```

```
plt.xlabel('Magnitude (Mw)')
plt.ylabel('number of counts/earthquakes')
plt.title("Histogram of Earthquakes' Magnitude in SEB")
plt.hist(dataSEB.mag, bins=30)
```

```
plt.xlabel('Time (year)')
plt.ylabel('number of counts/earthquakes')
plt.title("Histogram of Earthquakes' time in SEB")
plt.hist(dataSEB.time, bins=71)
```

HISTOGRAMS FOR THE COMPARISON OF DIFFERENT BRANCHES

Comparison of earthquakes' depths

```
plt.xlabel('depth (km)')
plt.ylabel('number of counts/earthquakes')
plt.title("Comparison of Earthquakes' depth")
plt.hist(dataWB.depth, bins=55, color='b')
plt.hist(dataMER.depth, bins=65, color='g')
plt.hist(dataEB.depth, bins=60, color='r')
plt.hist(dataSEB.depth, bins=45, color='y')
```

Comparison of earthquakes' magnitude

```
plt.xlabel('Magnitude (Mw)')
plt.ylabel('number of counts/earthquakes')
plt.title("Comparison of Earthquakes' Magnitude")
plt.hist(dataMER.mag, bins=37, color='g')
plt.hist(dataWB.mag, bins=46, color='b')
plt.hist(dataEB.mag, bins=35, color='r')
plt.hist(dataSEB.mag, bins=30, color='y')
```

Comparison of earthquakes' time

```
plt.xlabel('Time (year)')
plt.ylabel('number of counts/earthquakes')
plt.title("Comparison of Earthquakes' time")
plt.hist(dataWB.time, bins=112, color='b')
plt.hist(dataEB.time, bins=95, color='r')
plt.hist(dataMER.time, bins=116, color='g')
plt.hist(dataSEB.time, bins=71, color='y')
```

PLOTS OF DIFFERENT BI-VARIATE HISTOGRAMS IN THE ENTIRE EAR

Time-magnitude Bi-variate histogram

```
# Limit of the edges along both X and Y axis
t_min = np.min(data.time)
t_max = np.max(data.time)
mag_min = np.min(data.mag)
mag_max = np.max(data.mag)

# Creating the edges with varying numbers of bins along both X and
    Y axis
bin_X = 116
bin_Y = 44
Xedges = np.linspace(t_min,t_max,bin_X)
Yedges = np.linspace(mag_min,mag_max,bin_Y)

# Binning the number of events in (Xedges, Yedges)
Numb, Xedges, Yedges = np.histogram2d(data.time, data.mag, bins=(
    Xedges, Yedges))

# Building grid for positions of the 3d bars
X, Y = np.meshgrid(Xedges[:-1]+0.25, Yedges[:-1]+0.25, indexing="ij
    ")
X = X.ravel()
Y = Y.ravel()
Z = 0

# Defining bar properties Width, Length, Height
Const = 0.5 # constant adjusting the area of bar's Width*Length
Wid = Leng = Const*np.ones_like(Z)
Heig = Numb.ravel()

# Plotting
FIG = plt.figure(figsize=(7,6))
AX1 = FIG.add_subplot(111, projection='3d')
AX1.bar3d(X, Y, Z, Wid, Leng, Heig, shade=True)
#AX1.bar3d(X, Y, Z, Wid, Leng, Heig, color='b', shade=True) #
    Plotting with color
AX1.set_xlabel("Time (year)")
AX1.set_ylabel("Magnitude (Mw)")
AX1.set_zlabel("Number of counts/Earthquakes")
plt.show()
```

Depth-magnitude Bi-variate histogram

```
# Limit of the edges along both X and Y axis
dep_min = np.min(data.depth)
dep_max = np.max(data.depth)
mag_min = np.min(data.mag)
mag_max = np.max(data.mag)

# Creating the edges with varying numbers of bins along both X and Y axis
bin_X = 116
bin_Y = 44
Xedges = np.linspace(dep_min,dep_max,bin_X)
Yedges = np.linspace(mag_min,mag_max,bin_Y)

# Binning the number of events in (Xedges, Yedges)
Numb, Xedges, Yedges = np.histogram2d(data.depth, data.mag, bins=(Xedges,Yedges))

# Building grid for positions of the 3d bars
X, Y = np.meshgrid(Xedges[:-1]+0.25, Yedges[:-1]+0.25, indexing="ij")
X = X.ravel()
Y = Y.ravel()
Z = 0

# Defining bar properties Width, Length, Height
Const = 0.5 # constant adjusting the area of the bar's Width*Length
Wid = Leng = Const*np.ones_like(Z)
Heig = Numb.ravel()

# Plotting
FIG = plt.figure(figsize=(7,6))
AX1 = FIG.add_subplot(111, projection='3d')
AX1.bar3d(X, Y, Z, Wid, Leng, Heig, shade=True)
#AX1.bar3d(X, Y, Z, Wid, Leng, Heig, color='b', shade=True) # Plotting with color
AX1.set_xlabel("Depth (km)")
AX1.set_ylabel("Magnitude (Mw)")
AX1.set_zlabel("Number of counts/Earthquakes")
plt.show()
```

Depth-time Bi-variate histogram

```
# Limit of edges along both X and Y axis
dep_min = np.min(data.depth)
dep_max = np.max(data.depth)
t_min = np.min(data.time)
t_max = np.max(data.time)

# Creating the edges with varying numbers of bins along both X and
    Y axis
bin_X = 116
bin_Y = 116
Xedges = np.linspace(dep_min,dep_max,bin_X)
Yedges = np.linspace(t_min,t_max,bin_Y)

# Binning the number of events in (Xedges, Yedges)
Numb, Xedges, Yedges = np.histogram2d(data.depth, data.time, bins=(
    Xedges,Yedges))

# Building grid for positions of the 3d bars
X, Y = np.meshgrid(Xedges[:-1]+0.25, Yedges[:-1]+0.25, indexing="ij
    ")
X = X.ravel()
Y = Y.ravel()
Z = 0

# Defining bar properties Width, Length, Height
Const = 1.0 # constant adjusting the area of the bar's Width*Length
Wid = Leng = Const*np.ones_like(Z)
Heig = Numb.ravel()

# Plotting
FIG = plt.figure(figsize=(7,6)) # Adjusting the size of the figure
AX1 = FIG.add_subplot(111, projection='3d')
AX1.bar3d(X, Y, Z, Wid, Leng, Heig, shade=True)
#AX1.bar3d(X, Y, Z, Wid, Leng, Heig, color='b', shade=True) #
    Plotting with color
AX1.set_xlabel("Depth (km)")
AX1.set_ylabel("Time (year)")
AX1.set_zlabel("Number of counts/Earthquakes")
plt.show()
```

Time-latitude Bi-variate histogram

```
# Limits of the edges along both X and Y axis
t_min = np.min(data.time)
t_max = np.max(data.time)
lat_min = np.min(data.latitude)
lat_max = np.max(data.latitude)

# Creating the edges with varying numbers of bins along both X and Y axis
bin_X = 116
bin_Y = 116
Xedges = np.linspace(t_,in,t_max,bin_X)
Yedges = np.linspace(lat_min, lat_max,bin_Y)

# Binning the number of events in (Xedges,Yedges)
Numb, Xedges, Yedges = np.histogram2d(data.time, data.latitude, bins=(Xedges,Yedges))

# Building grid for positions of the 3d bars
X, Y = np.meshgrid(Xedges[:-1]+0.25, Yedges[:-1]+0.25, indexing="ij")
X = X.ravel()
Y = Y.ravel()
Z = 0

# Defining bar properties Width, Length, Height
Const = 0.5 # constant adjusting the area of the bar's Width*Length
Wid = Leng = Const*np.ones_like(Z)
Heig = Numb.ravel()

# Plotting
FIG = plt.figure(figsize=(7,6)) # Adjusting the size of the figure
AX1 = FIG.add_subplot(111, projection='3d')
AX1.bar3d(X, Y, Z, Wid, Leng, Heig, shade=True)
#AX1.bar3d(X, Y, Z, Wid, Leng, Heig, color='b', shade=True) # Plotting with color
AX1.set_xlabel("Time (year)")
AX1.set_ylabel("Latitude (Degrees)")
AX1.set_zlabel("Number of counts/Earthquakes")
plt.show()
```

Longitude-latitude Bi-variate histogram

```
# Limit of the edges along both X and Y axis
Long_min = np.min(data.longitude)
Long_max = np.max(data.longitude)
Lat_min = np.min(data.latitude)
Lat_max = np.max(data.latitude)

# Creating the edges with varying numbers of bins along both X and Y axis
bin_X = 116
bin_Y = 116
Xedges = np.linspace(Long_min,Long_max,bin_X)
Yedges = np.linspace(Lat_min,Lat_max,bin_Y)

# Binning the number of events in (Xedges, Yedges)
Numb, Xedges, Yedges = np.histogram2d(data.longitude, data.latitude, bins=(Xedges, Yedges))

# Building grid for position of the 3d bars
X, Y = np.meshgrid(Xedges[:-1]+0.25, Yedges[:-1]+0.25, indexing="ij")
X = X.ravel()
Y = Y.ravel()
Z = 0

# Defining bar properties Width, Length, Height
Const = 0.5 # constant adjusting the area of the bar's Width*Length
Wid = Leng = Const*np.ones_like(Z)
Heig = Numb.ravel()

# Plotting
FIG = plt.figure(figsize=(7,6)) # Adjusting the size of the figure
AX1 = FIG.add_subplot(111, projection='3d')
AX1.bar3d(X, Y, Z, Wid, Leng, Heig, shade=True)
#AX1.bar3d(X, Y, Z, Wid, Leng, Heig, color='b', shade=True) # Plotting with color
AX1.set_xlabel("Longitude (Degrees)")
AX1.set_ylabel("Latitude (Degrees)")
AX1.set_zlabel("Number of counts/Earthquakes")
plt.show()
```

CALCULATION OF THE MEAN, STANDARD DEVIATION, SKEWNESS AND KURTOSIS OF THE EARTHQUAKES' MAGNITUDE

a. In the entire East African Region

```
print('The mean of Magnitude is', stats.mean(data.mag)

print('The standard deviation of magn is', stats.stdev(data.mag))

data.skew(axis=0)

data.kurtosis(axis=0)
```

b. In the Western Branch

```
print('The mean of Magnitude is', stats.mean(dataWB.mag))

print('The standard deviation of magn is', stats.stdev(dataWB.mag))

dataWB.skew(axis=0)

dataWB.kurtosis(axis=0)
```

c. In the Eastern Branch

```
print('The mean of Magnitude is', stats.mean(dataEB.mag))

print('The standard deviation of magn is', stats.stdev(dataEB.mag))

dataEB.skew(axis=0)

dataEB.kurtosis(axis=0)
```

d. In the Main Ethiopian Rift

```
print('The mean of Magnitude is', stats.mean(dataMER.mag))

print('The standard deviation of magn is', stats.stdev(dataMER.mag)
    )

dataMER.skew(axis=0)
dataMER.kurtosis(axis=0)
```

e. In the Southeastern Branch

```
print('The mean of Magnitude is', stats.mean(dataSEB.mag))

print('The standard deviation of magn is', stats.stdev(dataSEB.mag)
    )

dataSEB.skew(axis=0)
dataSEB.kurtosis(axis=0)
```

References

[1] Ayele, A., Jacques, E., Kassim, M., Kidane, T., Omar, A., Tait, S., Nercessian, A., de Chabalier, J.-B., and King, G. (2007). The volcano–seismic crisis in afar, ethiopia, starting september 2005. *Earth and Planetary Science Letters*, 255(1-2):177–187.

[2] Ayele, A. and Kulhánek, O. (1997). Spatial and temporal variations of seismicity in the horn of africa from 1960 to 1993. *Geophysical Journal International*, 130(3):805–810.

[3] Binks, R. and Fairhead, J. (1992). A plate tectonic setting for mesozoic rifts of west and central africa. *Tectonophysics*, 213(1-2):141–151.

[4] Bosworth, W. (1985). Geometry of propagating continental rifts. *Nature*, 316(6029):625–627.

[5] Burov, E. B. and Diament, M. (1995). The effective elastic thickness (t e) of continental lithosphere: what does it really mean? *Journal of Geophysical Research: Solid Earth*, 100(B3):3905–3927.

[6] Chorowicz, J. (2005). The east african rift system. *Journal of African Earth Sciences*, 43(1-3):379–410.

[7] Chorowicz, J., Fournier, J. L., and Vidal, G. (1987). A model for rift development in eastern africa. *Geological Journal*, 22(S2):495–513.

[8] Civiero, C., Goes, S., Hammond, J. O., Fishwick, S., Ahmed, A., Ayele, A., Doubre, C., Goitom, B., Keir, D., Kendall, J. M., et al. (2016). Small-scale thermal upwellings under the northern east african rift from s travel time tomography. *Journal of Geophysical Research: Solid Earth*, 121(10):7395–7408.

[9] Déverchère, J., Petit, C., Gileva, N., Radziminovitch, N., Melnikova, V., and San'Kov, V. (2001). Depth distribution of earthquakes in the baikal rift system and its implications for the rheology of the lithosphere. *Geophysical Journal International*, 146(3):714–730.

[10] Ebinger, C., Crow, M., Rosendahl, B., Livingstone, D., and LeFournier, J. (1984). Structural evolution of lake malaŵi, africa. *Nature*, 308(5960):627–629.

[11] Ebinger, C. J., Rosendahl, B., and Reynolds, D. (1987). Tectonic model of the malaŵi rift, africa. *Tectonophysics*, 141(1-3):215–235.

[12] Ebinger, C. J. and Sleep, N. (1998). Cenozoic magmatism throughout east africa resulting from impact of a single plume. *Nature*, 395(6704):788–791.

[13] Fairhead, J. and Stuart, G. (1982). The seismicity of the east african rift system and comparison with other continental rifts. *Continental and Oceanic Rifts*, 8:41–61.

[14] Gill, R. R. (1972). *The seismicity of east Africa*. PhD thesis, Durham University.

[15] Gorshkov, G. (1963). The seismicity of africa. *A review of the Natural Resources of the African Continent*, pages 101–151.

[16] Gouin, P. (1979). *Earthquake history of Ethiopia and the Horn of Africa*. IDRC, Ottawa, ON, CA.

[17] Gutenberg, B. and Richter, C. (1954). Seismicity of the world and associated phenomena.

[18] Hassan, R., Williams, S. E., Gurnis, M., and Müller, D. (2020). East african topography and volcanism explained by a single, migrating plume. *Geoscience Frontiers*.

[19] Hofstetter, R. and Beyth, M. (2003). The afar depression: interpretation of the 1960–2000 earthquakes. *Geophysical Journal International*, 155(2):715–732.

[20] Jakovlev, A., Rümpker, G., Schmeling, H., Koulakov, I., Lindenfeld, M., and Wallner, H. (2013). Seismic images of magmatic rifting beneath the western branch of the east african rift. *Geochemistry, Geophysics, Geosystems*, 14(11):4906–4920.

[21] Keir, D., Ebinger, C., Stuart, G., Daly, E., and Ayele, A. (2006). Strain accommodation by magmatism and faulting as rifting proceeds to breakup: Seismicity of the northern ethiopian rift. *Journal of Geophysical Research: Solid Earth*, 111(B5).

[22] Keir, D., Hamling, I. J., Ayele, A., Calais, E., Ebinger, C., Wright, T. J., Jacques, E., Mohamed, K., Hammond, J. O., Belachew, M., et al. (2009). Evidence for focused magmatic accretion at segment centers from lateral dike injections captured beneath the red sea rift in afar. *Geology*, 37(1):59–62.

[23] Koptev, A., Burov, E., Calais, E., Leroy, S., Gerya, T., Guillou-Frottier, L., and Cloetingh, S. (2016). Contrasted continental rifting via plume-craton interaction: Applications to central east african rift. *Geoscience Frontiers*, 7(2):221–236.

[24] Lapins, S., Kendall, J. M., Ayele, A., Wilks, M., Nowacki, A., and Cashman, K. V. (2020). Lower-crustal seismicity on the eastern border faults of the main ethiopian rift. *Journal of Geophysical Research: Solid Earth*, 125(8):e2020JB020030.

[25] Le Fournier, J., Chorowicz, J., TIERCELIN, J.-J., THOUIN, C., and BALZER, F. (1985). Le bassin du lac tanganyika: évolution tectonique et sédimentaire. *Comptes rendus de l'Académie des sciences. Série 2, Mécanique, Physique, Chimie, Sciences de l'univers, Sciences de la Terre*, 301(14):1053–1058.

[26] Lowrie, W. (2007). Fundamentals of geophysics, cambridge university press. *New York, USA*.

[27] Mohr, P. (1983). The morton-black hypothesis for the thinning of continental crust—revisited in western afar. In *Developments in Geotectonics*, volume 19, pages 509–528. Elsevier.

[28] Molnar, P. and Aggarwal, Y. P. (1971). A microearthquake survey in kenya. *Bulletin of the Seismological Society of America*, 61(1):195–201.

[29] Mougenot, D., Recq, M., Virlogeux, P., and Lepvrier, C. (1986). Seaward extension of the east african rift. *Nature*, 321(6070):599–603.

[30] Nwankwo, C. and Ettah, A. (2019). Characteristics of earthquakes along the east african rift and the mid-atlantic ridge. *World Scientific News*, 120(2):60–80.

[31] Oliva, S., Ebinger, C., Wauthier, C., Muirhead, J., Roecker, S., Rivalta, E., and Heimann, S. (2019). Insights into fault-magma interactions in an early-stage continental rift from source mechanisms and correlated volcano-tectonic earthquakes. *Geophysical Research Letters*, 46(4):2065–2074.

[32] Plummer, C. C., Carlson, D. H., Hammersley, L., et al. (2016). *Physical geology*. New York, NY: McGraw-Hill/Education, Inc.,.

[33] Strecker, M., Blisniuk, P., and Eisbacher, G. (1990). Rotation of extension direction in the central kenya rift. *Geology*, 18(4):299–302.

[34] Tobin, D. G., Ward, P. L., and Drake, C. L. (1969). Microearthquakes in the rift valley of kenya. *Geological Society of America Bulletin*, 80(10):2043–2046.

[35] Wadge, G., Biggs, J., Lloyd, R., and Kendall, J.-M. (2016). Historical volcanism and the state of stress in the east african rift system. *Frontiers in Earth Science*, 4:86.

[36] Zhao, D. (2001). Seismic structure and origin of hotspots and mantle plumes. *Earth and Planetary Science Letters*, 192(3):251–265.

[37] Zhao, D., Lei, J., Inoue, T., Yamada, A., and Gao, S. S. (2006). Deep structure and origin of the baikal rift zone. *Earth and Planetary Science Letters*, 243(3-4):681–691.